Na[GeF₅]·2HF: the first quarternary phase in the H–Na–Ge–F system

Valentin Bockmair,* Constantin Hoch, Irina Schusterbauer and Andreas J. Kornath‡

Department Chemie, Ludwig-Maximilians Universität München, Butenandtstrasse 5-13 (Haus D), D-81377 München, Germany. *Correspondence e-mail: valentin.bockmair@cup.uni-muenchen.de

Edited by M. Yousufuddin, University of North Texas at Dallas, USA

This article is dedicated to the memory of Professor Dr Andreas J. Kornath who passed away in March 2024.

‡ Deceased

The structure of *cis*- or *trans*-bridged [GeF₅]⁻ anionic chains have been investigated [Mallouk *et al.* (1984). *Inorg. Chem.* **23**, 3160–3166] showing the first crystal structures of μ-F-bridged pentafluorogermanates. Herein, we report the second crystal structure of *trans*-pentafluorogermanate anions present in the crystal structure of sodium *trans*-pentafluorogermanate(IV) bis(hydrogen fluoride), Na[GeF₅]·2HF. The crystal structure [orthorhombic $Pca2_1$, a = 12.3786 (3), b = 7.2189 (2), c = 11.4969 (3) Å and Z = 8] is built up from infinite chains of *trans*-linked [GeF₆]²⁻ octahedra, extending along the b axis and spanning a network of pentagonal bipyramidal distorted Na-centred polyhedra. These [NaF₇] polyhedra are linked in a *trans*-edge fashion *via* hydrogen fluoride molecules, in analogy to already known sodium hydrogen fluorides and potassium hydrogen fluorides.

1. Introduction

Superacid chemistry can be applied as a powerful tool to isolate reactive volatile species by the formation of salts (Bayer *et al.*, 2022; Leitz *et al.*, 2018, 2019). These salts are mainly stabilized by F-atom interactions and are therefore more stable compared with the starting material. Furthermore, this offers the opportunity to estimate the acidity of compounds and structural parameters while widely retaining molecular corpus (Seelbinder *et al.*, 2010).

Experiments and quantum chemical calculations revealed that the protonation of thiosulfuric acid is successful in the superacidic system HF/MF_5 (M = As, Sb) (Hopfinger *et al.*, 2018). Investigations of the less acidic binary superacidic system HF/GeF₄ were performed to explore the structural chemistry of thiosulfuric acid and its protonated species. Since the H_0 value of the binary superacidic system HF/GeF₄ was assumed to be only slightly greater than for HF/AsF₅-based systems, monoprotonation was expected.

It turned out that the reaction of sodium thiosulfate in HF/GeF₄ led to the formation of Na[GeF₅]·2HF instead of protonation of thiosulfuric acid (see Scheme 1). Whereas no conversion of the sodium salts with the weakly coordinating anions [AsF₆]⁻ and [SbF₆]⁻ has been observed, the Lewis acid GeF₄ reacts with the formation of its sodium salt, *i.e.* Na[GeF₅].

The obtained compound Na[GeF₅]·2HF is the first quaternary phase in the Na–Ge–H–F system. The crystal structure shows an unusual pentagonal bipyramidal coordination of Na by F, in analogy to IF₇ (Burbank, 1962; Christe *et al.*, 1993). A similar coordination environment has not been observed for sodium yet, even for the related sodium hydrogen fluorides (Ivlev *et al.*, 2017). The sodium hydrogen fluorides also
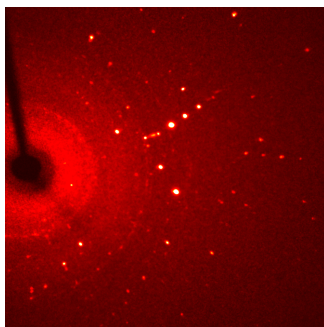
consists of μ-HF-linked polyhedra, such as the potassium hydrogen fluorides (Coyle *et al.*, 1969, 1970).

$$Na_2S_2O_3 \xrightarrow[233\ K]{HF/GeF_4} 2\ Na[GeF_5] + H_2S_2O_3$$
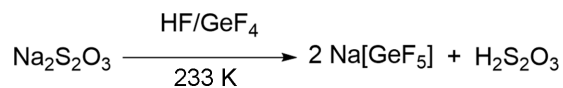
Scheme 1

There is a rich structural diversity of $[GeF_6]^{2-}$-based anions which can be classified in analogy to silicates. The main differences are the octahedral coordination of germanium and connections of $[GeF_6]^{2-}$ units *via* corners and edges. The most common anions are isolated, such as $[GeF_6]^{2-}$ (neso), $[Ge_2F_{10}]^{2-}$ (soro) or $[Ge_3F_{16}]^{4-}$. Octahedra chains of the anion can also be linked *via* *cis* or *trans* linkage, *i.e.* $\{[GeF_5]^-\}_n$, in analogy to inosilicates or can even form loop-branched chains, *i.e.* $\{[Ge_4F_{19}]^{3-}\}_n$ (Soltner, 2011). $Na[GeF_5]\cdot 2HF$ shows the rather rare structure element of *trans*-connected chains of pentafluorogermanates, similar to $[XeF_5][GeF_5]$, the only representative so far documented by crystal structure analysis (Mallouk *et al.*, 1984).

2. Experimental

Caution! Note that any contact with the described compounds should be avoided. Hydrolysis of GeF$_4$ and the synthesized salts forms HF which burns skin and causes irreparable damage. Safety precautions should be taken while handling these compounds. All reactions were carried out by employing standard Schlenk techniques on a stainless steel vacuum line. The syntheses of the salts were performed using FEP/PFA (fluoroethylenepropylene/perfluoralkoxy) reactors with stainless steel valves.

2.1. Synthesis and crystallization

Anhydrous hydrogen fluoride (80.04 mg, 4.0 mmol) and germanium tetrafluoride (297.16 mg, 2.0 mmol) were condensed into an FEP reactor. The solution was warmed to 233 K and thoroughly mixed for 5 min. Sodium thiosulfate (158.11 mg, 1.0 mmol) was added to the superacid after freezing it at liquid nitrogen temperature, and the solution was warmed to 233 K again and thoroughly mixed for 5 min. The volatile components were removed over a period of 12 h *in vacuo* at 195 K. The product was obtained as colourless crystals in quantitative yield.

2.2. Crystal structure refinement

Basic crystallographic data and details of the data collection and structure refinement are summarized in Table 1. The positions of the H atoms in the structure were localized in the difference Fourier map and refined without any restrictions (Table 1). Symmetry checks by *ADDSYM* (Spek, 2001, 2003; Le Page, 1988) supported the space groups *Pbca* and *Pca*2$_1$ when regarding the heavy-atom arrangement; however, the noncentrosymmetric space group was only supported when taking the F and H atoms into account, as shown in Fig. 1. In contrast to the H and F atoms, the Na and Ge atoms contribute
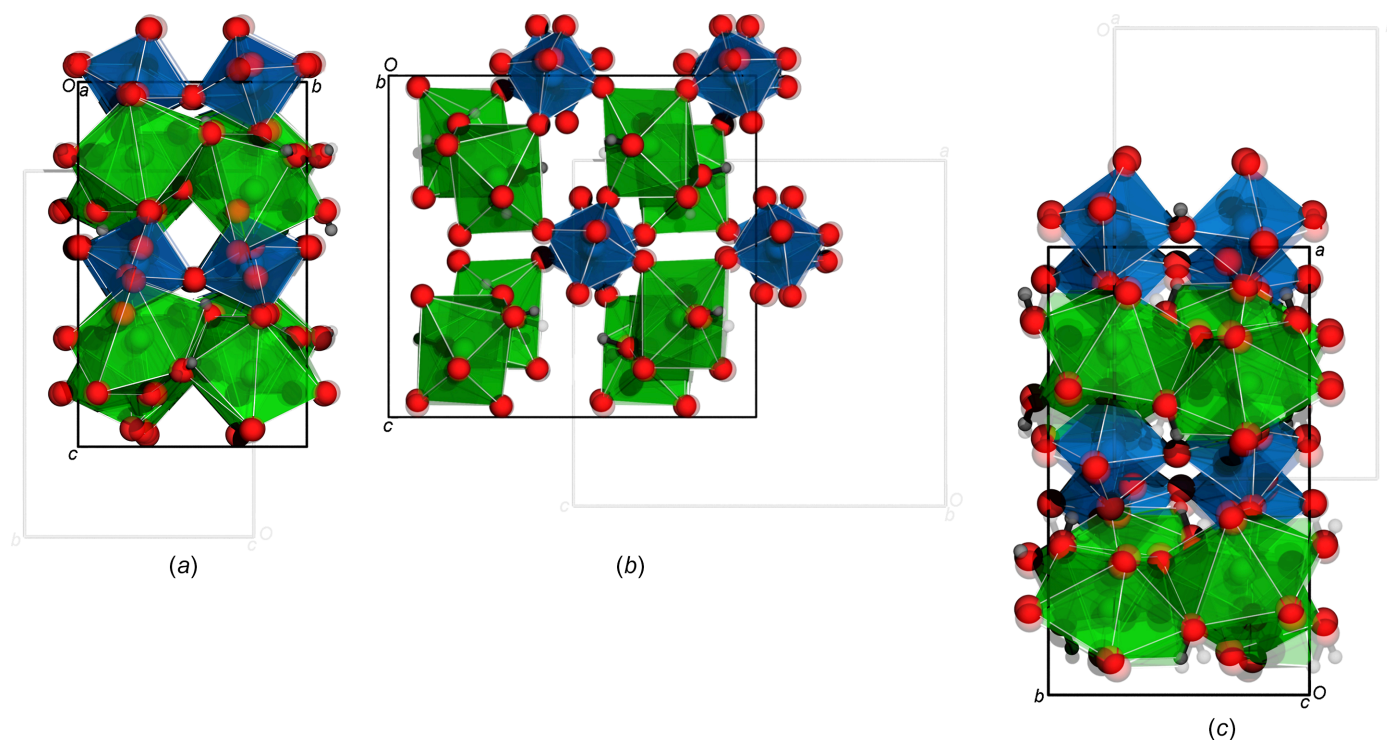

Figure 1
Overlay of the structural models in *Pca*2$_1$ and *Pbca* (light-grey unit cell, lighter atoms), viewed along (*a*) the *a* axis, (*b*) the *b* axis and (*c*) the *c* axis. Only H and F atoms show distinct differences in their respective positions, justifying the noncentrosymmetric model.

Table 1
Experimental details.

Crystal data	
Chemical formula	Na[GeF$_5$]·2HF
M_r	230.60
Crystal system, space group	Orthorhombic, $Pca2_1$
Temperature (K)	117
a, b, c (Å)	12.3786 (3), 7.2189 (2), 11.4969 (3)
V (Å^3)	1027.36 (5)
Z	8
Radiation type	Mo $K\alpha$
μ (mm^{-1})	6.12
Crystal size (mm)	0.39 × 0.27 × 0.20
Data collection	
Diffractometer	Rigaku Xcalibur Sapphire3
Absorption correction	Multi-scan (*CrysAlis PRO*; Rigaku OD, 2020)
T_{min}, T_{max}	0.566, 1.000
No. of measured, independent and observed [$I > 2\sigma(I)$] reflections	19491, 3147, 2948
R_{int}	0.020
$(\sin \theta/\lambda)_{max}$ (Å^{-1})	0.714
Refinement	
$R[F^2 > 2\sigma(F^2)]$, $wR(F^2)$, S	0.016, 0.041, 1.06
No. of reflections	3147
No. of parameters	180
No. of restraints	1
H-atom treatment	All H-atom parameters refined
$\Delta\rho_{max}$, $\Delta\rho_{min}$ (e Å^{-3})	0.35, −0.42
Absolute structure	Refined as an inversion twin
Absolute structure parameter	0.482 (13)

Computer programs: *CrysAlis PRO* (Rigaku OD, 2020), *SHELXT* (Sheldrick, 2015a), *SHELXL2018* (Sheldrick, 2015b), *ORTEP-3 for Windows* (Farrugia, 2012) and *PLATON* (Spek, 2020).

to hypersymmetry. The structure was refined as an inversion twin.

The calculated moiety formula was adjusted from 'F20 Ge4, 8(F H), 4(Na)' with $Z = 2$ to 'Na Ge F5, 2(F H)' with $Z = 8$, since the space group is orthorhombic and all atoms occupy the general position 4a. Due to symmetry, it can also be seen that the chains of octahedra are not isolated [Ge$_2$F$_{10}$]$^{2-}$ but instead {[GeF$_5$]$^-$}$_n$ units.

2.3. Analysis

The product was further analysed by low-temperature vibrational spectroscopy in order to confirm the conformation of the fluorogermanate anion. IR spectroscopic investigations were carried out with a Bruker Vertex-80V FT–IR spectrometer using a cooled cell with a single-crystal CsBr plate on which small amounts of the sample were placed (Bayersdorfer *et al.*, 1972). For the Raman measurements, a Bruker MultiRam FT–Raman spectrometer with Nd:YAG laser excitation ($\lambda = 1064$ nm) was used. The measurement was performed after transferring the sample into a cooled (77 K) glass cell under a nitrogen atmosphere and subsequent evacuation of the glass cell. The low-temperature spectra are depicted in Fig. 2.

Single crystals of Na[GeF$_5$]·2HF suitable for single-crystal diffraction analysis were selected under a stereomicroscope in a cooled nitrogen stream. The single crystal was prepared on a stainless steel polyamide micromount (see Fig. 3) and data collection was performed at 117 K on a Xcalibur diffractometer system (Rigaku Oxford Diffraction). For details of the data collection and treatment, as well as of the structure solution and refinement, see the supporting information.

Decomposition of the product was already identified at 238 K by detecting the development of vapour pressure with temperature.

3. Results and discussion

3.1. Vibrational spectroscopy

The Raman spectra show a broad line (712–600 cm^{-1}) appearing at 665 cm^{-1} for the terminal Ge—F vibration of the [GeF$_5$]$^-$ anion (654 and 622 cm^{-1}) [the frequencies in parentheses are from Mallouk *et al.* (1984)]. The Ge—F stretching vibrations of the $_\infty^1$[GeF$_5$]$^-$ chain appear at between 536 and 524 cm^{-1} (526 and 518 cm^{-1}). The bands at 388 (381), 336 (339) and 329 cm^{-1} (331 cm^{-1}) can be assigned
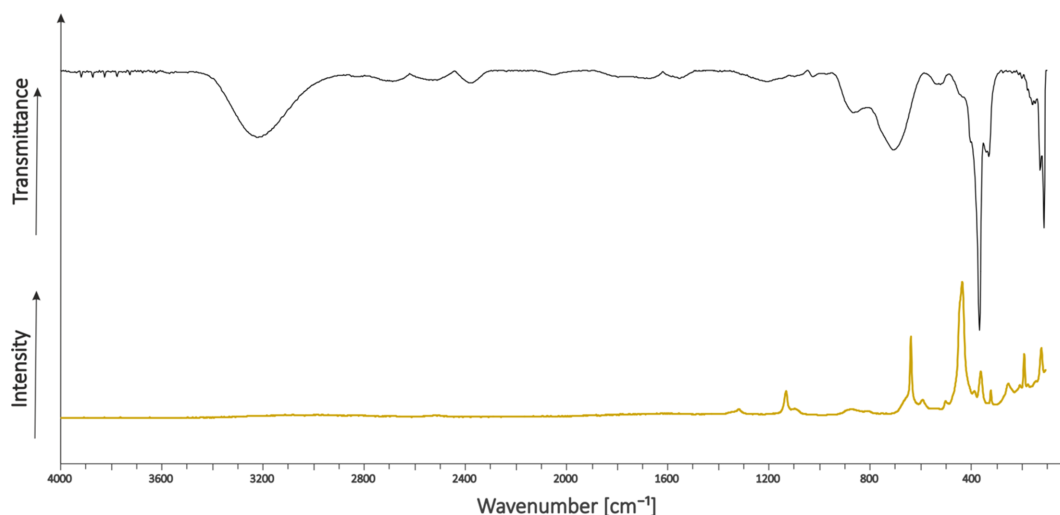

Figure 2
Vibrational spectra of Na[GeF$_5$]·2HF, showing IR (top) and Raman (bottom).

Table 2
Vibrational assignments for Na[GeF$_5$]·2HF (frequencies in cm^{-1}).

Abbreviations for IR intensities: v = very, s = strong, m = medium, w = weak. Experimental Raman activities are relative to a scale of 1 to 100.

Raman	IR	Raman (literature)	IR (literature)	Assignment
	758 (w)		746 (s)	ν_{as} NaF$_2$ axial
		676 (2)		ν_s NaF$_2$ axial
665 [100, vs (broad)]		654		ν_s [GeF$_5$]$_n$ terminal
		635 (10)		ν_s NaF$_5$ axial
		622		ν_{as} [GeF$_5$]$_n$ terminal
	657 (w)		670 (vs)	ν_{as} NaF$_5$ equatorial
	596 (s)	596 (0.2)		mixture δ sciss of NaF$_5$ in-plane
536 (18, w)		526		ν [GeF$_5$]$_n$ chain
524 (19, w)		518		ν [GeF$_5$]$_n$
	403 (w)		425 (vs)	δ_{as} NaF$_5$ in-plane
388 (24, w)		381		δ [GeF$_5$]$_n$ equatorial
	374 (w)		365 (s)	δ umbrella NaF$_5$ equatorial
	358 (m)		365 (s)	δ umbrella NaF$_5$ equatorial
336 (26, w)		339		δ [GeF$_5$]$_n$
329 (26, w)		329		δ [GeF$_5$]$_n$

to the square-plane angle deformation modes. These vibrations are similar to the values reported by Mallouk *et al.*
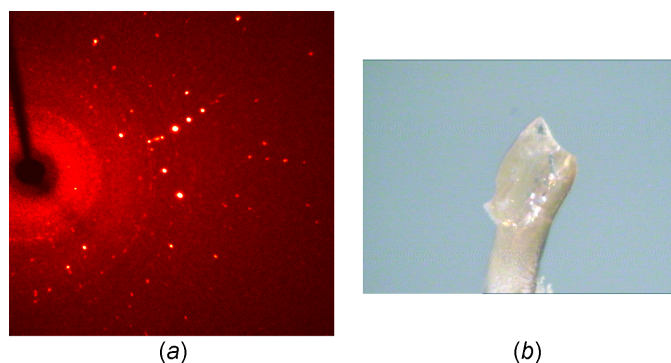

Figure 3
(a) Diffraction pattern and (b) the prepared single crystal on a polyamide loop of the micromount.
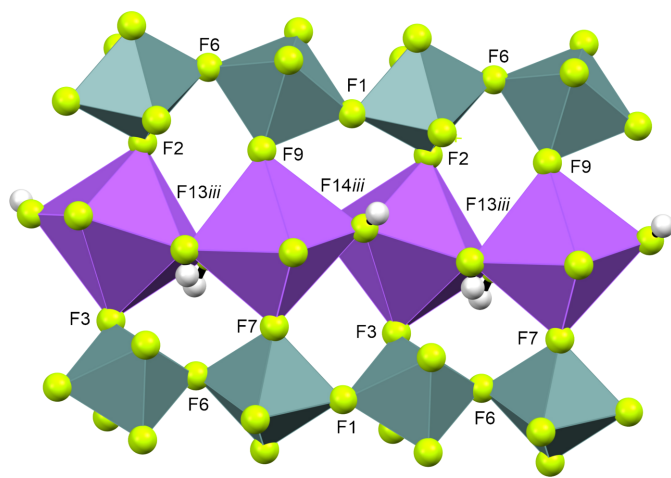

Figure 4
Structural cut-out of the crystal structure of Na[GeF$_5$]·2HF, viewed along the *a* axis. Na-centred and Ge-centred polyhedra are shown in purple and grey, respectively. [Symmetry codes: (i) $-x, -y, z - \frac{1}{2}$; (ii) $x + \frac{1}{2}, -y, -z + \frac{1}{2}$; (iii) $-x + \frac{1}{2}, y, z + \frac{1}{2}$.]

(1984), but the data suffers from overlap in the fingerprint area.

The IR spectra reveal the existence of hydrogen fluoride by its rotation bands at high wavenumbers (3921, 3879, 3834 3788, 3742, 3693 and 3643 cm^{-1}). In addition, the [NaF$_7$] polyhedra show bands similar to the structurally related IF$_7$ (Christe *et al.*, 1993) that can be found at 758 (746), 657 (670), 403 (425), 374 and 358 cm^{-1} (365 cm^{-1}).

The lines at 1342 [ν(SO$_3$)] and 1158 cm^{-1} [ν(SO$_2$)] are due to the decomposition of the solvent (H$_2$S$_2$O$_3$) according to Scheme 2, as are the bands at 3269 [ν(OH)], 1067 [ν(SO)] and 916 cm^{-1} [ν(SF)]. It can be assumed that the sulfur dioxide released by the decomposition of thiosulfuric acid reacts with excess hydrogen fluoride to form fluorosulfinic acid, as well as traces of polythionic acids, as reported in the literature (Hopfinger *et al.*, 2018).

Scheme 2
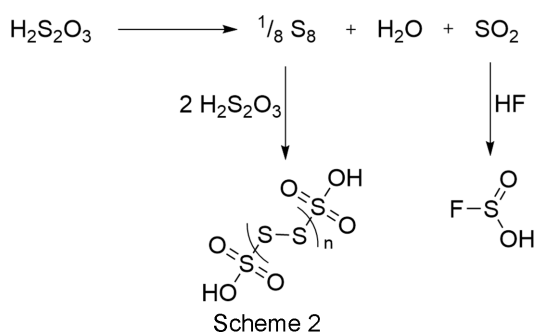
Since the structural chemistry of fluorogermanates has not been fully understood, other anions, as calculated by Soltner (2011), were compared with the observed data. Therefore, vibrations were also assigned to [GeF$_5$]$^-$ in accordance with the literature. The final assignments of vibrations for Na-[GeF$_5$]·2HF are listed in Table 2.

3.2. Crystal structure

In the $_\infty^1$[GeF$_5$]$^-$ chains (Figs. 4 and 5), the *trans*-connected [GeF$_6$]$^{2-}$ octahedra are tilted 28.94° with respect to each

Table 3
Structural comparison of Ge—F bond lengths (Å).

Na[GeF₅]·2HF (This work)		[XeF₅][GeF₅] (Mallouk *et al.*, 1984)		[(Me₂OH)₂][Ge₂F₁₀] (Soltner, 2011)	
Ge1—F1	1.8752 (15)	Ge—F1	1.745 (2)	Ge1—F1	1.7918 (12)
Ge1—F2	1.7719 (17)	Ge—F2	1.745 (2)	Ge1—F2	1.7393 (12)
Ge1—F3	1.741 (2)	Ge—F3	1.890 (1)	Ge1—F3	1.7450 (12)
Ge1—F4	1.770 (2)			Ge1—F4	1.7426 (12)
Ge1—F5	1.750 (2)			Ge1—F5	1.9128 (12)
Ge1—F6	1.8711 (15)			Ge1—F5′	1.9515 (12)
Ge2—F7	1.751 (2)				
Ge2—F8	1.765 (2)				
Ge2—F9	1.736 (2)				
Ge2—F10	1.745 (2)				
Ge2—F1ⁱ	1.8923 (15)				

Symmetry code: (i) x, y + 1, z.

other, and the octahedra are connected by atoms F1 and F6 (Fig. 6). The chains are arranged along the *b* axis and bent at Ge—F—Ge by 146.19°, forming zigzag chains. The octahedra are formed by atoms F1–F6 for Ge1 and F6–F10 for Ge2. The nonbridging Ge—F bonds are in the range 1.736 (2)–1.7719 (17) Å, in contrast to the bridging F atoms, which have a range of 1.8711 (15)–1.9020 (16) Å between Ge1 and Ge2. The atomic coordinates, anisotropic displacement parameters and interatomic distances and angles are compiled in the supporting information. The [GeF₅]⁻ units in Na[GeF₅] show similar Ge—F bond lengths to those in [XeF₅][GeF₅], but are slightly different due to distortion (Table 3).

The sodium ions exhibit an unusual distorted pentagonal bipyramidal coordination. The coordination spheres of Na1 and Na2 are built up from atoms F2–F4 belonging to one *trans*-pentafluorogermanate anion and from F7, F9 and F10 from the second *trans*-pentafluorogermanate anion, and four F

Figure 6
The coordination environments of Ge1 and Ge2. Displacement ellipsoids are displayed at the 50% probability level.

atoms (F11–F14) belonging to HF molecules (Fig. 7). The μ-F-bridged Na1- and Na2-centred polyhedra are *trans*-edge-linked, forming an infinite tilted chain extended along the *b* axis. The distances between Na1 and Na2 are 3.906 (2) and 3.934 (2) Å, respectively, and the Na—F distances range from 2.271 (2) to 2.610 (3) Å. Therefore, Na[GeF₅]·2HF displays similar Na—F distances, but with higher deviations, compared to NaH₄F₅ (Table 4). The different distances of the μ-HF bridges leads to distortion of the pentagonal bipyramid by the germanium chains.
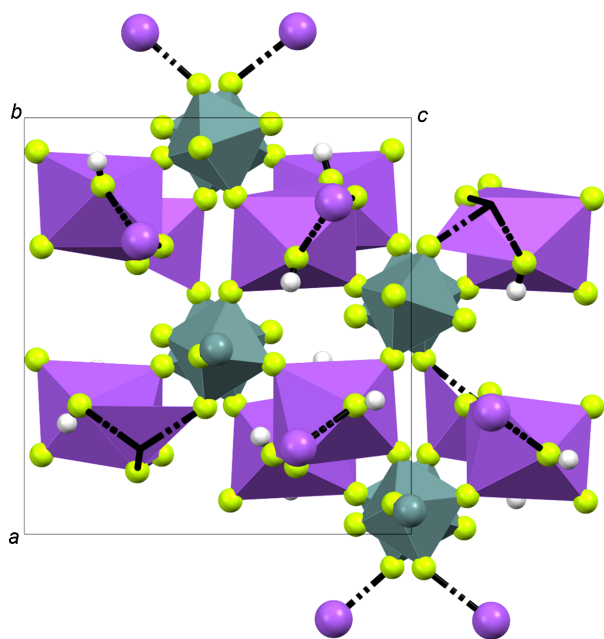

Figure 5
The crystal structure of Na[GeF₅]·2HF, viewed along the *b* axis. Na-centred and Ge-centred polyhedra are shown in purple and grey, respectively.
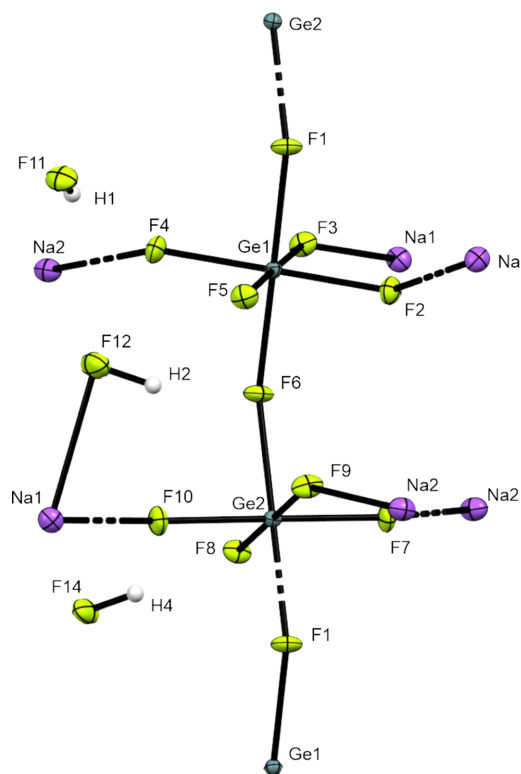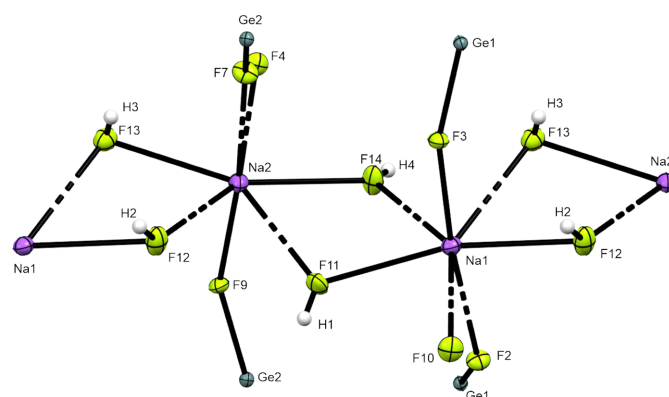

Figure 7
The coordination environments of Na1 and Na2. Displacement ellipsoids are displayed at the 50% probability level.

Table 4
Structural comparison of Na—F interatomic distances (Å).

Na[GeF$_5$]·2HF		NaH$_4$F$_5$ (Ivlev *et al.*, 2017)	
Na1—F3	2.271 (2)	Na—F2	2.4337 (5)
Na1—F10^{ii}	2.333 (3)	Na—F2	2.5104 (4)
Na1—F12	2.337 (2)		
Na1—F2^{iii}	2.348 (3)		
Na1—F11	2.359 (2)		
Na1—F14^{iv}	2.385 (2)		
Na1—F13^{iii}	2.610 (3)		
Na2—F9	2.236 (2)		
Na2—F7^{v}	2.252 (3)		
Na2—F14	2.334 (2)		
Na2—F13	2.373 (2)		
Na2—F12^{v}	2.431 (2)		
Na2—F11^{vi}	2.500 (3)		
Na2—F4^{vii}	2.557 (3)		

Symmetry codes: (ii) $-x + 1, -y + 1, z + \frac{1}{2}$; (iii) $-x + \frac{3}{2}, y, z + \frac{1}{2}$; (iv) $-x + \frac{3}{2}, y - 1, z + \frac{1}{2}$; (v) $-x + \frac{3}{2}, y, z - \frac{1}{2}$; (vi) $-x + \frac{3}{2}, y + 1, z - \frac{1}{2}$; (vii) $-x + 1, -y + 1, z - \frac{1}{2}$.

Two very strong hydrogen bonds are formed, namely, F12—H2···F5 [2.499 (3) Å] and F14—H4···F8 [2.483 (3) Å]. Two medium-strong hydrogen bonds form the connections F11—H1···F4 [2.661 (3) Å] and F13—H3···F2 [2.637 (3) Å]. Weaker interactions are F13—H3···F7 [3.007 (3) Å], F11—H1···F7 [2.895 (3) Å], F11—H1···F10 [2.870 (3) Å], F14—H4···F5 [3.105 (3) Å] and F12—H2···F8 [3.173 (3) Å]. The given distances are derived from F···F interatomic distances. In accordance with the criteria given by Jeffrey (1997), the assignment of weak/strong hydrogen bonds shows short and directed contacts for strong and longer and nondirectional contacts for weaker hydrogen bonds.

4. Conclusion

Thiosulfuric acid could not be protonated in the superacidic system HF/GeF$_4$ as intended. However, thiosulfuric acid proved to be a solvent for the crystallization of new $A[Ge_xF_y]_z$ salts (A = alkali or alkaline-earth metals) due to the balanced acidity, volatility and extraordinary solubility of fluorine-containing metal salts. By exploiting this method, new structures of alkali or alkaline-earth fluorogermanates might become accessible.

Expanding the gaps between the infinitive chains might result in new structures or might cause conformational changes in the fluorogermanate chains. Following this procedure, the structural chemistry of fluorogermantes could become more comprehensive. In analogy to silicates, ring formation might be observed in compounds with large low-charged cations.

It may also be possible to synthesize Na[GeF$_5$] in a simplified reaction of sodium fluoride in HF/GeF$_4$ and it may be possible to improve the spectroscopic data, as decomposition of the solvent (H$_2$S$_2$O$_3$) could be avoided. Since the investigations were originally aimed at the protonation of thiosulfuric acid, no futher attempt was made to figure out whether the presence of thiosulfuric acid is necessary as a solvent or if the reaction could also just succeed in anhydrous hydrogen fluoride. As the solubility of sodium hydrogen fluorides increases drastically in anhydrous hydrogen fluoride

with higher hydrogen fluoride content at low temperature, it can be expected that without additional solvent the reaction needs to be heated to homogenize the product. Otherwise a mixture of NaH$_4$F$_5$ and NaF may be obtained reacting with the Lewis acid GeF$_4$, leading to a mixture of different Na[GeF$_5$]·nHF.

Furthermore, the levelling effect of sodium salts could be shown for GeF$_4$-based systems, in analogy to BF$_3$ decreasing Lewis acidity under the formation of sodium salts.

References

Bayer, M. C., Greither, N., Bockmair, V., Nitzer, A. & Kornath, A. J. (2022). *Eur. J. Inorg. Chem.* **2022**, e202200501.

Bayersdorfer, L., Minkwitz, R. & Jander, J. (1972). *Z. Anorg. Allge Chem.* **392**, 137–142.

Burbank, R. D. (1962). *Acta Cryst.* **15**, 1207–1214.

Christe, K. O., Curtis, E. C. & Dixon, D. A. (1993). *J. Am. Chem. Soc.* **115**, 1520–1526.

Coyle, B. A., Schroeder, L. W. & Ibers, J. A. (1969). *Acta Cryst.* A**25**, s114.

Coyle, B. A., Schroeder, L. W. & Ibers, J. A. (1970). *J. Solid State Chem.* **1**, 386–393.

Farrugia, L. J. (2012). *J. Appl. Cryst.* **45**, 849–854.

Hopfinger, M., Zischka, F., Seifert, M. & Kornath, A. J. (2018). *Z. Anorg. Allge Chem.* **644**, 574–579.

Ivlev, S. I., Soltner, T., Karttunen, A., Mühlbauer, M., Kornath, A. J. & Kraus, F. (2017). *Z. Anorg. Allge Chem.* **643**, 1436–1443.

Jeffrey, G. A. (1997). In *An Introduction to Hydrogen Bonding*, in *Topics in Physical Chemistry*. New York: Oxford University Press.

Leitz, D., Nitzer, A., Morgenstern, Y., Zischka, F. & Kornath, A. J. (2019). *Eur. J. Inorg. Chem.* **2019**, 808–812.

Leitz, D., Stierstorfer, K., Morgenstern, Y., Zischka, F. & Kornath, A. J. (2018). *Z. Anorg. Allge Chem.* **644**, 483–488.

Le Page, Y. (1988). *J. Appl. Cryst.* **21**, 983–984.

Mallouk, T. E., Desbat, B. & Bartlett, N. (1984). *Inorg. Chem.* **23**, 3160–3166.

Rigaku OD (2020). *CrysAlis PRO*. Rigaku Oxford Diffraction Ltd, Yarnton, Oxfordshire, England.

Seelbinder, R., Goetz, N. R., Weber, J., Minkwitz, R. & Kornath, A. J. (2010). *Chem. Eur. J.* **16**, 1026–1032.

Sheldrick, G. M. (2015*a*). *Acta Cryst.* A**71**, 3–8.

Sheldrick, G. M. (2015*b*). *Acta Cryst.* C**71**, 3–8.

Soltner, T. (2011). PhD thesis, Ludwig-Maximilian University, Munich, Bavaria, Germany.

Spek, A. L. (2001). PhD thesis, Utrecht University, Utrecht, Netherlands.

Spek, A. L. (2003). *J. Appl. Cryst.* **36**, 7–13.

Spek, A. L. (2020). *Acta Cryst.* E**76**, 1–11.

supporting information

Na[GeF₅]·2HF: the first quarternary phase in the H–Na–Ge–F system

Valentin Bockmair, Constantin Hoch, Irina Schusterbauer and Andreas J. Kornath

Computing details

Sodium *trans*-pentafluorogermanate(IV) bis(hydrogen fluoride)

Crystal data

Na[GeF₅]·2HF	D_x = 2.982 Mg m⁻³
M_r = 230.60	Mo $K\alpha$ radiation, λ = 0.71073 Å
Orthorhombic, $Pca2_1$	Cell parameters from 7284 reflections
a = 12.3786 (3) Å	θ = 2.4–32.3°
b = 7.2189 (2) Å	μ = 6.12 mm⁻¹
c = 11.4969 (3) Å	T = 117 K
V = 1027.36 (5) Å³	Block, colorless
Z = 8	0.39 × 0.27 × 0.20 mm
$F(000)$ = 864	

Data collection

Rigaku Xcalibur Sapphire3 diffractometer	19491 measured reflections
Radiation source: Enhance (Mo) X-ray Source	3147 independent reflections
Graphite monochromator	2948 reflections with $I > 2\sigma(I)$
Detector resolution: 15.9809 pixels mm⁻¹	R_{int} = 0.020
ω scans	θ_{max} = 30.5°, θ_{min} = 3.3°
Absorption correction: multi-scan (CrysAlis PRO; Rigaku OD, 2020)	$h = -17 \rightarrow 17$
	$k = -10 \rightarrow 10$
	$l = -16 \rightarrow 16$
T_{min} = 0.566, T_{max} = 1.000	

Refinement

Refinement on F^2	Secondary atom site location: difference Fourier map
Least-squares matrix: full	Hydrogen site location: difference Fourier map
$R[F^2 > 2\sigma(F^2)]$ = 0.016	All H-atom parameters refined
$wR(F^2)$ = 0.041	$w = 1/[\sigma^2(F_o^2) + (0.021P)^2 + 0.1191P]$ where $P = (F_o^2 + 2F_c^2)/3$
S = 1.06	
3147 reflections	$(\Delta/\sigma)_{max}$ = 0.001
180 parameters	$\Delta\rho_{max}$ = 0.35 e Å⁻³
1 restraint	$\Delta\rho_{min}$ = −0.41 e Å⁻³
Primary atom site location: structure-invariant direct methods	Absolute structure: Refined as an inversion twin
	Absolute structure parameter: 0.482 (13)

Special details

Geometry. All esds (except the esd in the dihedral angle between two l.s. planes) are estimated using the full covariance matrix. The cell esds are taken into account individually in the estimation of esds in distances, angles and torsion angles; correlations between esds in cell parameters are only used when they are defined by crystal symmetry. An approximate (isotropic) treatment of cell esds is used for estimating esds involving l.s. planes.

Refinement. Refinement of F^2 against ALL reflections. The weighted R-factor wR and goodness of fit S are based on F^2, conventional R-factors R are based on F, with F set to zero for negative F^2. The threshold expression of $F^2 > 2\mathrm{sigma}(F^2)$ is used only for calculating R-factors(gt) etc. and is not relevant to the choice of reflections for refinement. R-factors based on F^2 are statistically about twice as large as those based on F, and R- factors based on ALL data will be even larger.
Refined as a 2-component inversion twin.

Fractional atomic coordinates and isotropic or equivalent isotropic displacement parameters (Å^2)

	x	y	z	U_{iso}*/U_{eq}
Ge2	0.55613 (2)	0.75939 (3)	0.49576 (2)	0.00657 (7)
Ge1	0.55679 (2)	0.25939 (3)	0.50121 (2)	0.00684 (7)
Na1	0.70406 (10)	0.23808 (15)	0.79934 (17)	0.0128 (3)
Na2	0.70770 (11)	0.74018 (16)	0.20626 (17)	0.0137 (3)
F13	0.69103 (15)	0.4287 (3)	0.1429 (2)	0.0171 (4)
F4	0.41887 (15)	0.2182 (2)	0.5324 (2)	0.0141 (4)
F3	0.59190 (16)	0.2076 (2)	0.64417 (18)	0.0131 (4)
F8	0.51440 (13)	0.8257 (2)	0.63655 (17)	0.0127 (3)
F2	0.69427 (13)	0.3009 (2)	0.4672 (2)	0.0139 (4)
F14	0.66327 (16)	1.0544 (3)	0.2028 (2)	0.0191 (4)
F1	0.57251 (14)	0.01177 (19)	0.4549 (2)	0.0129 (3)
F6	0.53956 (13)	0.5083 (2)	0.5426 (2)	0.0139 (4)
F5	0.52321 (14)	0.3129 (2)	0.35719 (18)	0.0134 (3)
F12	0.65158 (16)	0.5488 (2)	0.7918 (2)	0.0203 (4)
F9	0.59674 (15)	0.6946 (2)	0.35709 (18)	0.0144 (4)
F7	0.69007 (15)	0.7564 (2)	0.5446 (2)	0.0146 (4)
F10	0.42153 (16)	0.7636 (2)	0.4507 (2)	0.0162 (4)
F11	0.69129 (15)	−0.0757 (3)	0.8549 (2)	0.0175 (4)
H4	0.605 (3)	1.090 (4)	0.188 (3)	0.004 (7)*
H1	0.679 (3)	−0.106 (5)	0.905 (4)	0.020 (11)*
H3	0.734 (6)	0.442 (8)	0.110 (8)	0.13 (3)*
H2	0.583 (7)	0.506 (10)	0.770 (8)	0.21 (4)*

Atomic displacement parameters (Å^2)

	U^{11}	U^{22}	U^{33}	U^{12}	U^{13}	U^{23}
Ge2	0.00698 (14)	0.00612 (12)	0.00660 (16)	0.00019 (7)	0.00006 (14)	−0.00005 (16)
Ge1	0.00725 (14)	0.00598 (13)	0.00729 (17)	−0.00031 (7)	−0.00050 (14)	0.00057 (16)
Na1	0.0139 (6)	0.0141 (6)	0.0103 (7)	0.0012 (4)	−0.0011 (5)	−0.0012 (5)
Na2	0.0174 (7)	0.0117 (6)	0.0121 (7)	0.0009 (4)	0.0031 (6)	0.0005 (5)
F13	0.0172 (10)	0.0166 (10)	0.0176 (12)	−0.0017 (7)	0.0004 (7)	−0.0020 (9)
F4	0.0094 (8)	0.0169 (7)	0.0161 (9)	−0.0027 (6)	0.0017 (7)	0.0002 (7)
F3	0.0170 (9)	0.0134 (8)	0.0089 (9)	−0.0021 (7)	−0.0029 (7)	0.0010 (7)
F8	0.0176 (9)	0.0121 (8)	0.0086 (8)	0.0018 (7)	0.0032 (7)	−0.0008 (7)

F2	0.0107 (8)	0.0171 (8)	0.0139 (9)	−0.0006 (6)	0.0025 (6)	−0.0008 (8)
F14	0.0166 (9)	0.0137 (8)	0.0270 (11)	0.0032 (7)	−0.0108 (8)	−0.0003 (8)
F1	0.0215 (8)	0.0059 (7)	0.0112 (8)	0.0000 (5)	0.0009 (8)	0.0009 (6)
F6	0.0214 (9)	0.0062 (7)	0.0141 (9)	0.0010 (5)	0.0044 (8)	0.0006 (6)
F5	0.0167 (9)	0.0139 (8)	0.0095 (8)	−0.0003 (7)	−0.0020 (7)	0.0021 (7)
F12	0.0201 (10)	0.0148 (8)	0.0260 (11)	0.0020 (7)	0.0083 (8)	−0.0016 (9)
F9	0.0222 (10)	0.0124 (7)	0.0086 (9)	−0.0019 (7)	0.0038 (7)	−0.0023 (7)
F7	0.0077 (8)	0.0201 (9)	0.0160 (9)	0.0002 (5)	−0.0025 (6)	0.0019 (7)
F10	0.0098 (8)	0.0188 (8)	0.0199 (9)	0.0005 (6)	−0.0046 (7)	0.0006 (8)
F11	0.0227 (10)	0.0147 (9)	0.0150 (12)	0.0000 (7)	0.0058 (7)	0.0041 (9)

Geometric parameters (Å, º)

Ge2—F9	1.736 (2)	Na1—F12	2.337 (2)
Ge2—F10	1.745 (2)	Na1—F2^{iii}	2.348 (3)
Ge2—F7	1.751 (2)	Na1—F11	2.359 (2)
Ge2—F8	1.765 (2)	Na1—F14^{iv}	2.385 (2)
Ge2—F1^{i}	1.8923 (15)	Na1—F13^{iii}	2.610 (3)
Ge2—F6	1.9020 (16)	Na1—Na2^{iv}	3.9060 (19)
Ge1—F3	1.741 (2)	Na1—Na2^{iii}	3.9340 (19)
Ge1—F5	1.750 (2)	Na2—F9	2.236 (2)
Ge1—F4	1.770 (2)	Na2—F7^{v}	2.252 (3)
Ge1—F2	1.7719 (17)	Na2—F14	2.334 (2)
Ge1—F6	1.8711 (15)	Na2—F13	2.373 (2)
Ge1—F1	1.8752 (15)	Na2—F12^{v}	2.431 (2)
Na1—F3	2.271 (2)	Na2—F11^{vi}	2.500 (3)
Na1—F10^{ii}	2.333 (3)	Na2—F4^{vii}	2.557 (3)
F9—Ge2—F10	90.48 (11)	F13^{iii}—Na1—Na2^{iv}	99.04 (6)
F9—Ge2—F7	90.97 (11)	F3—Na1—Na2^{iii}	92.60 (6)
F10—Ge2—F7	178.54 (14)	F10^{ii}—Na1—Na2^{iii}	113.13 (6)
F9—Ge2—F8	179.78 (10)	F12—Na1—Na2^{iii}	35.19 (6)
F10—Ge2—F8	89.32 (10)	F2^{iii}—Na1—Na2^{iii}	84.07 (6)
F7—Ge2—F8	89.22 (11)	F11—Na1—Na2^{iii}	167.70 (6)
F9—Ge2—F1^{i}	90.03 (10)	F14^{iv}—Na1—Na2^{iii}	101.22 (6)
F10—Ge2—F1^{i}	90.66 (8)	F13^{iii}—Na1—Na2^{iii}	35.79 (5)
F7—Ge2—F1^{i}	89.42 (8)	Na2^{iv}—Na1—Na2^{iii}	134.08 (4)
F8—Ge2—F1^{i}	89.86 (9)	F9—Na2—F7^{v}	173.15 (9)
F9—Ge2—F6	91.98 (9)	F9—Na2—F14	90.65 (9)
F10—Ge2—F6	89.88 (8)	F7^{v}—Na2—F14	93.89 (9)
F7—Ge2—F6	89.98 (8)	F9—Na2—F13	92.59 (8)
F8—Ge2—F6	88.12 (10)	F7^{v}—Na2—F13	81.07 (9)
F1^{i}—Ge2—F6	177.91 (14)	F14—Na2—F13	153.53 (11)
F3—Ge1—F5	179.21 (10)	F9—Na2—F12^{v}	92.45 (9)
F3—Ge1—F4	90.76 (10)	F7^{v}—Na2—F12^{v}	87.76 (9)
F5—Ge1—F4	89.99 (9)	F14—Na2—F12^{v}	136.71 (10)
F3—Ge1—F2	90.30 (10)	F13—Na2—F12^{v}	69.39 (8)
F5—Ge1—F2	88.95 (10)	F9—Na2—F11^{vi}	81.68 (9)

F4—Ge1—F2	178.92 (13)	F7^{v}—Na2—F11^{vi}	104.81 (9)
F3—Ge1—F6	89.68 (10)	F14—Na2—F11^{vi}	67.22 (8)
F5—Ge1—F6	90.09 (9)	F13—Na2—F11^{vi}	139.22 (10)
F4—Ge1—F6	90.00 (8)	F12^{v}—Na2—F11^{vi}	70.57 (8)
F2—Ge1—F6	90.19 (8)	F9—Na2—F4^{vii}	104.30 (9)
F3—Ge1—F1	92.14 (9)	F7^{v}—Na2—F4^{vii}	72.12 (9)
F5—Ge1—F1	88.09 (10)	F14—Na2—F4^{vii}	74.23 (8)
F4—Ge1—F1	89.85 (8)	F13—Na2—F4^{vii}	79.52 (8)
F2—Ge1—F1	89.93 (8)	F12^{v}—Na2—F4^{vii}	145.28 (9)
F6—Ge1—F1	178.17 (14)	F11^{vi}—Na2—F4^{vii}	141.09 (8)
F3—Na1—F10^{ii}	100.25 (9)	F9—Na2—Na1^{vi}	95.44 (6)
F3—Na1—F12	83.91 (9)	F7^{v}—Na2—Na1^{vi}	91.21 (6)
F10^{ii}—Na1—F12	81.23 (8)	F14—Na2—Na1^{vi}	34.56 (6)
F3—Na1—F2^{iii}	172.69 (8)	F13—Na2—Na1^{vi}	168.67 (7)
F10^{ii}—Na1—F2^{iii}	75.25 (9)	F12^{v}—Na2—Na1^{vi}	102.23 (6)
F12—Na1—F2^{iii}	89.66 (9)	F11^{vi}—Na2—Na1^{vi}	35.28 (5)
F3—Na1—F11	94.53 (8)	F4^{vii}—Na2—Na1^{vi}	106.10 (5)
F10^{ii}—Na1—F11	75.41 (8)	F9—Na2—Na1^{v}	79.86 (6)
F12—Na1—F11	155.94 (10)	F7^{v}—Na2—Na1^{v}	96.69 (6)
F2^{iii}—Na1—F11	89.92 (9)	F14—Na2—Na1^{v}	164.87 (8)
F3—Na1—F14^{iv}	90.09 (9)	F13—Na2—Na1^{v}	40.05 (7)
F10^{ii}—Na1—F14^{iv}	143.40 (9)	F12^{v}—Na2—Na1^{v}	33.63 (5)
F12—Na1—F14^{iv}	135.07 (11)	F11^{vi}—Na2—Na1^{v}	99.50 (6)
F2^{iii}—Na1—F14^{iv}	96.93 (8)	F4^{vii}—Na2—Na1^{v}	119.41 (6)
F11—Na1—F14^{iv}	68.79 (8)	Na1^{vi}—Na2—Na1^{v}	134.08 (4)
F3—Na1—F13^{iii}	79.28 (8)	Na2—F13—Na1^{v}	104.17 (10)
F10^{ii}—Na1—F13^{iii}	148.00 (8)	Ge1—F4—Na2^{ii}	136.86 (11)
F12—Na1—F13^{iii}	66.85 (8)	Ge1—F3—Na1	150.86 (11)
F2^{iii}—Na1—F13^{iii}	101.40 (8)	Ge1—F2—Na1^{v}	131.60 (11)
F11—Na1—F13^{iii}	136.57 (10)	Na2—F14—Na1^{vi}	111.73 (10)
F14^{iv}—Na1—F13^{iii}	68.28 (8)	Ge1—F1—Ge2^{viii}	146.75 (14)
F3—Na1—Na2^{iv}	82.34 (6)	Ge1—F6—Ge2	146.18 (14)
F10^{ii}—Na1—Na2^{iv}	112.69 (6)	Na1—F12—Na2^{iii}	111.18 (9)
F12—Na1—Na2^{iv}	161.96 (8)	Ge2—F9—Na2	148.24 (11)
F2^{iii}—Na1—Na2^{iv}	104.65 (5)	Ge2—F7—Na2^{iii}	142.90 (14)
F11—Na1—Na2^{iv}	37.76 (7)	Ge2—F10—Na1^{vii}	149.04 (14)
F14^{iv}—Na1—Na2^{iv}	33.72 (5)	Na1—F11—Na2^{iv}	106.96 (11)
F3—Ge1—F4—Na2^{ii}	33.60 (14)	F3—Ge1—F6—Ge2	143.9 (2)
F5—Ge1—F4—Na2^{ii}	−146.17 (14)	F5—Ge1—F6—Ge2	−35.32 (19)
F6—Ge1—F4—Na2^{ii}	−56.08 (15)	F4—Ge1—F6—Ge2	−125.31 (19)
F1—Ge1—F4—Na2^{ii}	125.74 (14)	F2—Ge1—F6—Ge2	53.6 (2)
F4—Ge1—F3—Na1	−153.3 (2)	F10—Ge2—F9—Na2	131.1 (2)
F2—Ge1—F3—Na1	26.8 (2)	F7—Ge2—F9—Na2	−48.9 (2)
F6—Ge1—F3—Na1	−63.4 (2)	F1^{i}—Ge2—F9—Na2	40.5 (2)
F1—Ge1—F3—Na1	116.8 (2)	F6—Ge2—F9—Na2	−139.0 (2)
F3—Ge1—F2—Na1^{v}	142.99 (14)	F9—Ge2—F7—Na2^{iii}	−160.32 (16)
F5—Ge1—F2—Na1^{v}	−37.24 (13)	F8—Ge2—F7—Na2^{iii}	19.79 (16)

F6—Ge1—F2—Na1^v	−127.33 (14)	F1^i—Ge2—F7—Na2^{iii}	109.66 (17)
F1—Ge1—F2—Na1^v	50.85 (15)	F6—Ge2—F7—Na2^{iii}	−68.33 (17)
F3—Ge1—F1—Ge2^{viii}	35.6 (2)	F9—Ge2—F10—Na1^{vii}	−13.35 (18)
F5—Ge1—F1—Ge2^{viii}	−145.1 (2)	F8—Ge2—F10—Na1^{vii}	166.55 (18)
F4—Ge1—F1—Ge2^{viii}	−55.1 (2)	F1^i—Ge2—F10—Na1^{vii}	76.69 (19)
F2—Ge1—F1—Ge2^{viii}	125.9 (2)	F6—Ge2—F10—Na1^{vii}	−105.33 (19)

Symmetry codes: (i) x, $y+1$, z; (ii) $-x+1$, $-y+1$, $z+1/2$; (iii) $-x+3/2$, y, $z+1/2$; (iv) $-x+3/2$, $y-1$, $z+1/2$; (v) $-x+3/2$, y, $z-1/2$; (vi) $-x+3/2$, $y+1$, $z-1/2$; (vii) $-x+1$, $-y+1$, $z-1/2$; (viii) x, $y-1$, z.